Effect of PEG Corona Lengths on MR Relaxivity and Off-resonance Saturation Sensitivity of Superparamagnetic Polymeric Micelles

C. Khemtong[1], O. Togao[2], J. Ren[2], C. W. Kessinger[1], M. Takahashi[2], A. D. Sherry[2], and J. Gao[1]
[1]Simmons Comprehensive Cancer Center, University of Texas Southwestern Medical Center, Dallas, TX, United States, [2]Advanced Imaging Research Center, University of Texas Southwestern Medical Center, Dallas, TX, United States

Introduction

Despite several excellent advantages of MRI as a clinical imaging technique, its application in molecular imaging of cancer has been limited due to the poor sensitivity. Superparamagnetic nanoparticles have received considerable attention as molecular imaging probes with substantially higher molar relaxivities over small molecular T_1 agents. Several new imaging methods have been developed to enhance the specificity and sensitivity of MR imaging of superparamagnetic nanoparticles. Recently, we have combined an ultra-sensitive design of cancer-targeted superparamagnetic polymeric micelles (SPPM) and an off-resonance saturation (ORS) method to enhance the imaging efficacy of tumor biomarkers *in vivo*. Herein, we report the effect of PEG corona lengths on MR relaxivity and ORS sensitivity of SPPM.

Experimental Methods

1,2-Distearoyl-*sn*-glycero-3-phosphoethanolamine-*N*-methoxy-poly(ethylene glycol) (DSPE-PEG) with different PEG molecular weights (1, 2, 5 kD) were used to encapsulate Fe_3O_4 nanoparticles (SPIO, diameter 7±0.7 nm). The polymer to SPIO weight ratios were 25:1 to ensure encapsulation of one single SPIO nanoparticle per SPPM. Size distribution of SPPM nanoparticles was analyzed using dynamic light scattering (DLS) and transmission electron microscopy (TEM). Iron concentration of SPPM solutions were measured by atomic absorption spectroscopy using an established calibration curve. Each phantom sample was prepared by varying SPPM concentrations ranging from 25 μM to 1 mM Fe. All MRI experiments of phantoms were conducted on a 7T Varian small animal imager with a 40 mm i.d. Millipede coil. T_2 times of SPPM solutions were determined using a fast spin echo pulse sequence with TR=2s and TE ranging from 7 ms to 500 ms. ORS experiments were carried out using a spin echo (SE) pulse sequence (TR = 2 s; TE = 8.5 ms) modified by the addition of a frequency-selective Gaussian-shaped pre-saturation pulse. The phantoms were RF irradiated with a saturation B_1 power of 2.6 μT for 0.5 s. An ON (Mz) image was irradiated with a frequency offset of 3 ppm from the bulk water, while an OFF (Mz^0) image was irradiated with a frequency at 50 ppm from the bulk water signal. An ORS image was obtained by taking a division of ON and OFF image (Mz/Mz^0).

Results and Discussion

Using 7 nm SPIO, we prepared a series of SPPM with different corona lengths by using DSPE-PEG with different PEG molecular weights (Fig. 1a). TEM and DLS analyses confirmed the core-shell architecture and monodispersity of all SPPM formulations. Negative stained TEM images revealed that each SPPM nanoparticle contains only one SPIO (Fig. 1d-f). Average hydrodynamic diameters of SPPM with PEG lengths of 1, 2, and 5 kD were 16.3 ± 1.8, 16.4 ± 2.0, and 17.9 ± 2.4 nm, respectively. Longer PEG length led to larger average diameters of the resulting SPPM nanoparticles, however, the comparison is not statistically significant.

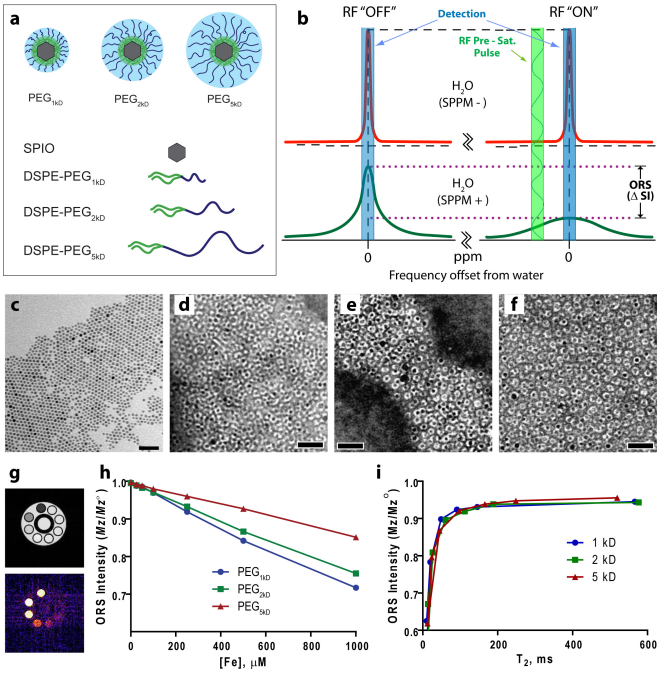

Figure 1. (a) A schematic representation of SPPM; (b) mechanism of SPPM-induced ORS contrast; (c) TEM of as-synthesized SPIO, (d-f) TEM of SPPM with PEG_{1kD}, PEG_{2kD}, PEG_{5kD} after staining with 2% PTA solution, respectively; (g) SE MR image of SPPM with PEG_{2kD} (top) and its $Mz/Mz°$ image (bottom). SPPM concentrations in the phantom are 25, 50, 100, 250, 500, and 1000 μM Fe, respectively.; (h) ORS intensity vs [SPPM], and (i) ORS intensity vs T_2.

MR relaxivity studies of phantom samples showed that the PEG length of SPPM greatly affects its T_2 relaxivity rate (r_2) in spite of containing identical SPIO. r_2 rates obtained at 7T were 171.5, 133.6, and 78.9 s^{-1} mM^{-1} Fe for SPPM with 1, 2, and 5 kD PEG corona, respectively. This is likely due to the shorter PEG corona of SPPM allows more surrounding water protons to diffuse into a close proximity of the superparmagnetic core of SPPM, thereby shortening their T_2 relaxation times. For ORS MRI, phantoms samples containing different SPPM concentrations were imaged using a pre-saturation pulse with a saturation power of 2.6 μT for 500 ms at 3 ppm from the bulk water signal. Spin echo MR images, obtained with RF saturation at 50 ppm (as OFF images) from the bulk water signal, showed Fe-induced image darkening trend in all three SPPM samples (see Fig. 1g, *top*, for example). The darkening of all SPPM concentrations became more pronounced when the saturation frequency was closer to the water peak (3 ppm). Image analysis showed that, at the same SPPM concentration, the contrast in ORS images was higher in the SPPM with shorter PEG corona (Fig. 1h). The ORS contrast also showed a linear relationship with SPPM concentration (shown here as per Fe concentration). The ORS sensitivity (slope) increased with decrease of PEG lengths, i.e., PEG_{1kD} > PEG_{2kD} > PEG_{5kD}. Further correlation of ORS contrast (Mz/Mz^0) vs. T_2 values of different SPPM samples shows that all three SPPM compositions demonstrated similar relationships (Fig. 1i), which indicates that T_2 value is the determinant factor for the ORS contrast. The ORS contrast becomes smaller as the T_2 value of SPPM solutions increased, reaching the plateau as T_2 values approaching the range of 100 ms.

Conclusion

In summary, we have prepared a series of SPPM with varied PEG corona lengths and studied their MR relaxivities and ORS sensitivity. Results showed that the length of the pegylated shell is a critical physical parameter that controls MR relaxivity and ORS sensitivity of SPPM. SPPM that has shorter PEG corona results in a higher MR relaxivity and hence ORS sensitivity. Results from this study provide the mechanistic insights on the ORS contrast sensitivity of SPPM nanoparticles, which assists the future development of SPPM as ultrasensitive MRI nanoprobes for *in vivo* imaging applications.

References

1. Khemtong et al *Cancer Res.* **2009**, 69, 1651-1658; 2. Zurkiya et al, *MRM.* **2006**, 56, 726.